The Venusian Atmospheric Oxygen Ion Escape: Extrapolation to the Early Solar System

M. Persson, Y. Futaana, R. Ramstad, K. Masunaga, H. Nilsson, M. Hamrin, A. Fedorov, S. Barabash

Key Points:
- The current escape of O^+ from Venus is energy limited not source limited
- The extrapolated mass loss through ion escape accounts for 6 mbar of the current Venusian atmosphere
- The total mass loss from ion escape cannot account for the loss of a large water inventory at Venus

Correspondence to:
M. Persson,
moa.persson@irf.se

The Venusian Atmospheric Oxygen Ion Escape: Extrapolation to the Early Solar System

M. Persson[1,2] , **Y. Futaana[1]** , **R. Ramstad[3]** , **K. Masunaga[3]** , **H. Nilsson[1]** , **M. Hamrin[2]** , **A. Fedorov[4], and S. Barabash[1]**

[1]Swedish Institute for Space Physics, Kiruna, Sweden, [2]Department of Physics, Umeå University, Umeå, Sweden, [3]Laboratory for Atmospheric and Space Physics, University of Colorado Boulder, Boulder, CO, USA, [4]IRAP, CNRS, Toulouse, France

Abstract The present atmosphere of Venus contains almost no water, but recent measurements indicate that in its early history, Venus had an Earth-like ocean. Understanding how the Venusian atmosphere evolved is important not only for Venus itself but also for understanding the evolution of other planetary atmospheres. In this study, we quantify the escape rates of oxygen ions from the present Venus to infer the past of the Venusian atmosphere. We show that an extrapolation of the current escape rates back in time leads to the total escape of 0.02–0.6 m of a global equivalent layer of water. This implies that the loss of ions to space, inferred from the present state, cannot account for the loss of an historical Earth-like ocean. We find that the O^+ escape rate increases with solar wind energy flux, where more energy available leads to a higher escape rate. Oppositely, the escape rate decreases slightly with increased extreme ultraviolet radiation (EUV) flux, though the small variation of EUV flux over the measured solar cycle may explain the weak dependency. These results indicate that there is not enough energy transferred from the solar wind to Venus' upper atmosphere that can lead to the escape of the atmosphere over the past 3.9 billion years. This means that the Venusian atmosphere did not have as much water in its atmosphere as previously assumed or the present-day escape rates do not represent the historical escape rates at Venus. Otherwise, some other mechanisms have acted to more effectively remove the water from the Venusian atmosphere.

Plain Language Summary Today, Venus only has small amounts of water in its atmosphere. In its early history, Venus presumably contained an Earth-like ocean of several meters. The evolution of the atmosphere may have been caused by escape of atmospheric content to space. In this study, we investigate how much the escape of oxygen ions to space could have affected the atmospheric evolution for Venus from measurements of the present-day escape rates. Using measurements of oxygen ions in the vicinity of Venus, we show that the amount of energy available in the solar wind to be transferred to the upper atmosphere of Venus determines how much of the atmosphere escapes. From the evolution of the energy in the solar wind over the past 3.9 billion years, together with the relation between the solar wind energy and oxygen ion escape, we show that in total, about 0.02–0.6 m of water depth, if spread equally over the entire Venusian surface, was lost. This indicates that either Venus did not have as much water as previously assumed or the current escape rates are not representative of the historical escape rates. Otherwise, some other mechanisms must have acted to more effectively remove the water from Venus.

1. Introduction

Today, the Venusian atmosphere is thick and dry and has a high CO_2 content, but it was likely different in its early history. Observations of the deuterium-to-hydrogen ratio and surface properties indicate that Venus had large amounts of water in its atmosphere billions of years ago (Donahue et al., 1997; Ingersoll, 1969; Taylor et al., 2018, and references therein). The high deuterium-to-hydrogen ratio indicate a fractionated long-term escape, where for example, the lighter hydrogen escapes easier than the heavier deuterium (Donahue et al., 1997). On the other hand, the observed high ratio may partly be explained by catastrophic resurfacing events and accompanied outgassing within the past 1 billion years, or large comet impacts which brings water with a high D/H ratio (Grinspoon, 1993; Taylor & Grinspoon, 2009). Even a combination of fractionated escape and the influx of water with a higher D/H ratio from either continuous or separate events may explain the current high D/H ratio (Donahue, 1999). Distinguishing between these different

interpretations is important for characterizing the evolution of the Venusian atmosphere. Therefore, it is important to determine the escape to space, how it affects the different species, particularly hydrogen and oxygen that composes water, and how it has evolved over time.

Billions of years ago, the solar extreme ultraviolet radiation (EUV) flux was 10–1000 times stronger than it is today (Ribas et al., 2005; Tu et al., 2015). The strong EUV flux would have significantly heated the atmosphere, expanded it, and caused a hydrodynamic escape of hydrogen to space, which by drag forces would have led to the escape of neutral oxygen (Gillmann & Tackley, 2014). Today, the thermal and hydrodynamical escape of neutral atoms to space is negligible, as the upper atmosphere of Venus is cooled by the CO_2 emissions in the upper atmosphere (Wordsworth & Pierrehumbert, 2013). Instead, the escape of neutral atoms comes mainly from the nonthermal escape through photochemical reactions and sputtering. The escape from photochemical reactions is only important for hydrogen, not O, due to the high escape energy for O (McElroy et al., 1982). Escape due to sputtering of neutral oxygen was estimated through modeling efforts to be on the order of 25% of the total ion escape rates today (Lammer et al., 2006) and has yet to be determined with measurements. Nevertheless, the neutral escape at present rates from the Venusian atmosphere is not a significant source for the atmospheric evolution.

On the other hand, the nonthermal ion escape mechanisms are important at Venus. Due to the lack of an intrinsic magnetic field, the ionosphere of Venus interacts directly with the solar wind. The incoming EUV radiation ionizes the upper atmospheric particles, which, if exposed to the solar wind, may get "picked up" by the motional electric field and escape in the magnetosheath (Luhmann et al., 2004). Ions created inside the induced magnetosphere may instead be transported to the nightside by a pressure gradient (Knudsen et al., 1980). The ions can then be accelerated above the escape velocity of around 10 km/s by either the ambipolar electric field, forming from the separation of heavy ions and lighter electrons, or the draped magnetic field in the magnetotail (Barabash et al., 2007; Collinson et al., 2016; Dubinin et al., 2011; Hartle & Grebowsky, 1990). A recent study by Masunaga et al. (2019) showed that less than 30% of oxygen ions escape through the pickup process in the magnetosheath, while the rest escapes through the induced magnetotail.

The Pioneer Venus Orbiter (PVO) mission estimated the escape rates when it orbited Venus during 1978–1992 (Colin, 1980). From measurements during 1979 to 1986, the electron altitude profiles in the nightside were determined to have an average density of 39 cm^{-3}, which together with the estimated average ion velocity equivalent to 13 eV, gave an average escaping flux of $5 \cdot 10^{25}$ O^+/s, if the average was assumed for the entire disk of Venus (Brace et al., 1987). This number could be an overestimation, as Venus Express (VEx) measurements later showed that the flux is mainly located in the central magnetotail and near the boundary region (Barabash, Fedorov, et al., 2007). Therefore, the estimated escape rates from Brace et al. (1987) should likely be divided by at least a factor 5 (Fedorov et al., 2011). Using magnetometer measurements in the magnetotail during 1979–1984 and assuming a simple draping pattern of magnetic fields in the Venusian magnetotail, McComas et al. (1986) calculated the plasma density, velocity, and temperature from the magnetohydrodynamic (MHD) momentum equation. The escape rate was estimated to $6 \cdot 10^{24}$ O^+/s. However, the time-averaged magnetic field draping in the Venusian magnetotail may be more asymmetrical (Zhang et al., 2010), and the escape rate may be an underestimation. Ion flow measurements near the equatorial terminators showed that there was a significant flow of O^+ across the terminator that is enough to sustain the nightside ionosphere of Venus (Knudsen et al., 1980). If assumed equal over the full disk of Venus it provides $5 \cdot 10^{26}$ O^+/s to the nightside that can potentially escape (Knudsen & Miller, 1992). The total flux is an upper limit, as the flow in the north pole terminator region has a significant dawn-to-dusk component in the flow in addition to its transterminator component (Persson et al., 2019). Nevertheless, the main portion of the ions flowing transterminator does not lead to escape as Venus does have a significant nightside ionosphere composed of gravitationally bound ions (Knudsen & Miller, 1992).

VEx measurements have shown that the total average escape rate from Venus today is $(3–6) \cdot 10^{24}$ O^+/s (see review by Futaana et al., 2017). The escape rates from VEx are thus lower than those found from the PVO measurements. This ambiguity may be explained by the difference in the upstream solar wind and solar parameters. From solar minimum to maximum, the O^+ escape rate tends to decrease slightly due to an increase in the Venusward fluxes in the near magnetotail, although the effect is strongest on the H^+ escape rate (Kollmann et al., 2016; Persson et al., 2018). On the other hand, during high dynamic pressure events,

the escape rates increase by a factor 1.9 (Edberg et al., 2011). In this study, we analyze the data from the full VEx mission during 2006–2014 to characterize the escape rate from the Venusian atmosphere with respect to the upstream parameters solar wind energy flux and solar EUV flux. We assume that the Venusian plasma environment responds systematically to the upstream conditions and can investigate the average state for each set of upstream parameters. The solar EUV flux was chosen since it is the main source of ion production. The increase in the EUV flux leads to an increase in the number of particles available in the ionosphere. The solar wind energy flux represents the amount of available energy in the solar wind and is directly related to the energy of the escaping particles. A part of the solar wind energy is transferred to the upper atmospheric particles which may lead to additional escape (Futaana et al., 2017). The purpose of this study is to find an empirical relation between the escape and these upstream parameters (section 3), which we then use for extrapolating the results backwards in time to calculate the total historical ion escape from the Venusian atmosphere (section 4).

2. Instrumentation and Method

We use data from the Ion Mass Analyzer (IMA), a part of the Analyser of Space Plasma and Energetic Atoms (ASPERA-4) instrument package on board VEx. IMA uses a top-hat electrostatic analyzer to differentiate the energy of the incoming ions in the range 0.01–36 keV with the energy resolution $E/E = 7\%$. The flying direction of the ion in the $360° \times 90°$ (~2π sr) field of view is resolved by 16 azimuthal sectors of 22.5° each and elevation deflector plates scanning the elevation plane over 16 (5.6° wide) steps. Each full ion distribution is sampled over angle and energy every 192 s. The mass per charge is differentiated for $M/Q = 1–44$ amu through an assembly of permanent magnets. The instrument is described in further detail by Barabash et al. (2007).

All measurements of IMA obtained from April 2006 to November 2014 are used to calculate the escape rate to estimate the O^+ outflow. The mass is separated as described in Fedorov et al. (2011), where the heaviest species are assumed to be O^+. The average escape rates are calculated by the method developed in Persson et al. (2018) with improvements to achieve acceptable statistics with the separation for different upstream parameters as outlined below.

In order to formulate the escape flux as a function of the solar wind energy flux and the solar extreme ultraviolet (EUV) flux, we first need to estimate these parameters. The upstream solar wind moments are calculated from H^+ flux distributions measured by IMA outside the Venusian bow shock on VEx inbound and outbound orbit segments. Distributions for which the expected solar wind incident flow direction (corrected for aberration) is outside the instrument field of view, or blocked by spacecraft surfaces, are excluded. The valid solar wind H^+ distributions measured outside the bow shock are subsequently integrated moment-wise over solid angle and energy (for $E > 100$ eV) to yield total solar wind H^+ densities and bulk velocities. Each O^+ measurement is then assigned the solar wind H^+ density and velocity that is closest in time within the same orbit period. As the full passage of the induced magnetosphere for VEx is short (around 2 hr), the expected deviation from the upstream solar wind at the exact time of O^+ measurement is small on a statistical basis.

VEx carried no dedicated instrument to monitor the solar EUV flux; instead, we estimate it using Earth-based measurements. We used the Solar EUV Experiment (SEE) on the Thermosphere Ionosphere Mesosphere Energetics Dynamics (TIMED) spacecraft (Woods et al., 2005). The TIMED/SEE measurements are propagated to the nearest point in time that Venus would have observed the same solar disk, accounting for the Carrington rotation period, and scaled in intensity to the Venusian heliocentric distance. The daily-averaged EUV irradiance from the solar disk is quasi-stable on timescales of several days, limited by a rotational modulation of 20% at 17–22 nm and 10% at longer wavelengths. Therefore, the typical error incurred from this propagation is estimated to be typically less than ~7% (Ramstad et al., 2018; Thiemann et al., 2017). When the Earth-Venus separation was $|\Delta L_S| < 45°$, the two planets are taken to have simultaneously observed roughly the same solar disk, as such we use TIMED/SEE observational (15 min) averages intensity scaled to Venus without propagation in time (Ramstad et al., 2018). Here, we define the EUV flux as wavelengths within 1–118 nm and integrate over wavelength to find the total solar EUV flux. The frequency distribution of the derived EUV flux and solar wind energy flux at Venus at the time of each IMA
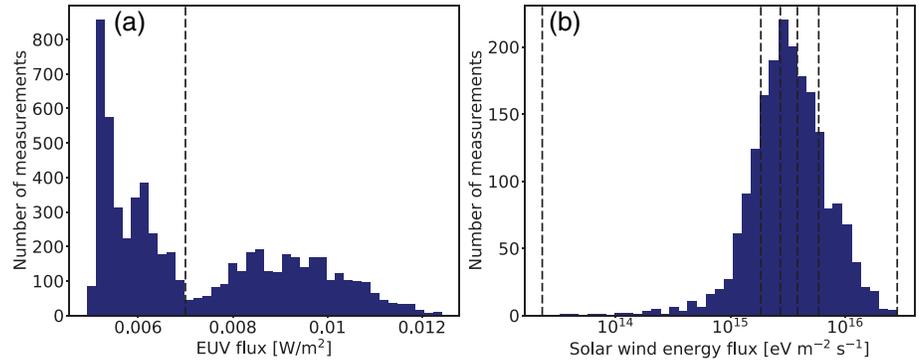
Figure 1. Frequency distributions of (a) the solar EUV flux at Venus, propagated from 1 A.U, separated into high and low condition at 0.007 Wm^{-2} (dashed line), and (b) the upstream solar wind energy flux calculated from the IMA measurements outside the bow shock of Venus, separated into five bins (dashed lines).

measurement is shown in Figure 1. The data are divided into two EUV flux conditions: high and low EUV, separated at 0.007 Wm^{-2}, and five solar wind energy flux bins within each solar EUV condition.

Average differential flux distributions are made from the O$^+$ measurements. Similar to Persson et al. (2018), the differential flux is organized by five degrees of freedom: two spatial dimensions (spacecraft position), two flying directions of the ions, and one for their energies. We used the Venus Solar Orbiter (VSO) cylindrical geometric frame to define the spatial bins. In the VSO frame, the X-axis points along the line from Venus to the Sun, and R is the distance from the X-axis. The cylindrical geometric frame is valid if we assume an axisymmetric magnetotail, ignoring any effects of the asymmetry along the solar wind motional electric field, $E_{mot} = -v_{sw} \times B_{IMF}$, where v_{sw} is the solar wind velocity and B_{IMF} is the interplanetary magnetic field (Jarvinen et al., 2013; McComas et al., 1986; Pérez-de-Tejada, 2001). As the sensitivity of the choice of frame for the escape rate calculations is small (Nordström et al., 2013), the assumption is deemed valid. The flying directions θ and φ of the ions are determined from the location of the VEx spacecraft at the time of the measurement, similar to Figure 1 in Ramstad et al. (2015). The elevation angle θ determines the radial velocity component, while the azimuth angle φ determines the velocity in the tangential-lateral plane.

Based on each upstream parameter, we separate the data set of IMA O$^+$ observations into 10 groups. For each group, we produce maps of O$^+$ flux (Figure 2). Here, the magnetotail of Venus is divided into spatial bins with $X = R = 0.3$ Rv (Rv = Venus radii = 6,052 km). The flux map $F_X(X_i, R_j)$ is obtained by integration of the five-dimensional differential flux $\overline{J}(X_i, R_j, \varphi_k, \theta_l, E_m)$ over the energy and angular dimensions.

$$F_x(X_i, R_j) = \int \overline{J}(X, R, \varphi, \theta, E) cos^2(\theta) cos(\varphi) d\varphi d\theta dE = \sum \overline{J}(X_i, R_j, \varphi_k, \theta_l, E_m) cos^2(\theta_l) cos(\varphi_k) \varphi \theta E_m. \quad (1)$$

The energy width E is computed so that the energy is divided as to be linearly distributed in velocity width with $v = 5$ km/s. The angular space is divided to have azimuth bin size of $\varphi = 7.2°$ and elevation bin size of $\theta = 3.6°$. The average differential flux $\overline{J}(X_i, R_j, \varphi_k, \theta_l, E_m)$ was calculated through an arithmetic mean of the measurements in each spatial bin for each upstream condition. Note that the differential flux $\overline{J}$, flying directions φ and θ, and energy E are here corrected for the spacecraft velocity.

Figure 2 shows examples of the total fluxes in the X_{VSO} direction in each spatial grid for the 10 chosen upstream conditions. In general, the fluxes are on average tailward (reddish bins), with a few bins with dominating Venusward flux (blueish bins). The Venusward flux is more prominent for the high solar EUV conditions, which agrees with the results that the return flows increase from solar minimum to solar maximum as reported in Persson et al. (2018). In addition, the number of bins with dominating Venusward fluxes decrease with increasing solar wind energy flux, specifically for the high EUV case. This is mainly due to an increase in energy of the O$^+$ out from the planet with increasing solar wind energy flux, where the Venusward flux does not change significantly over the changing solar wind energy flux conditions.
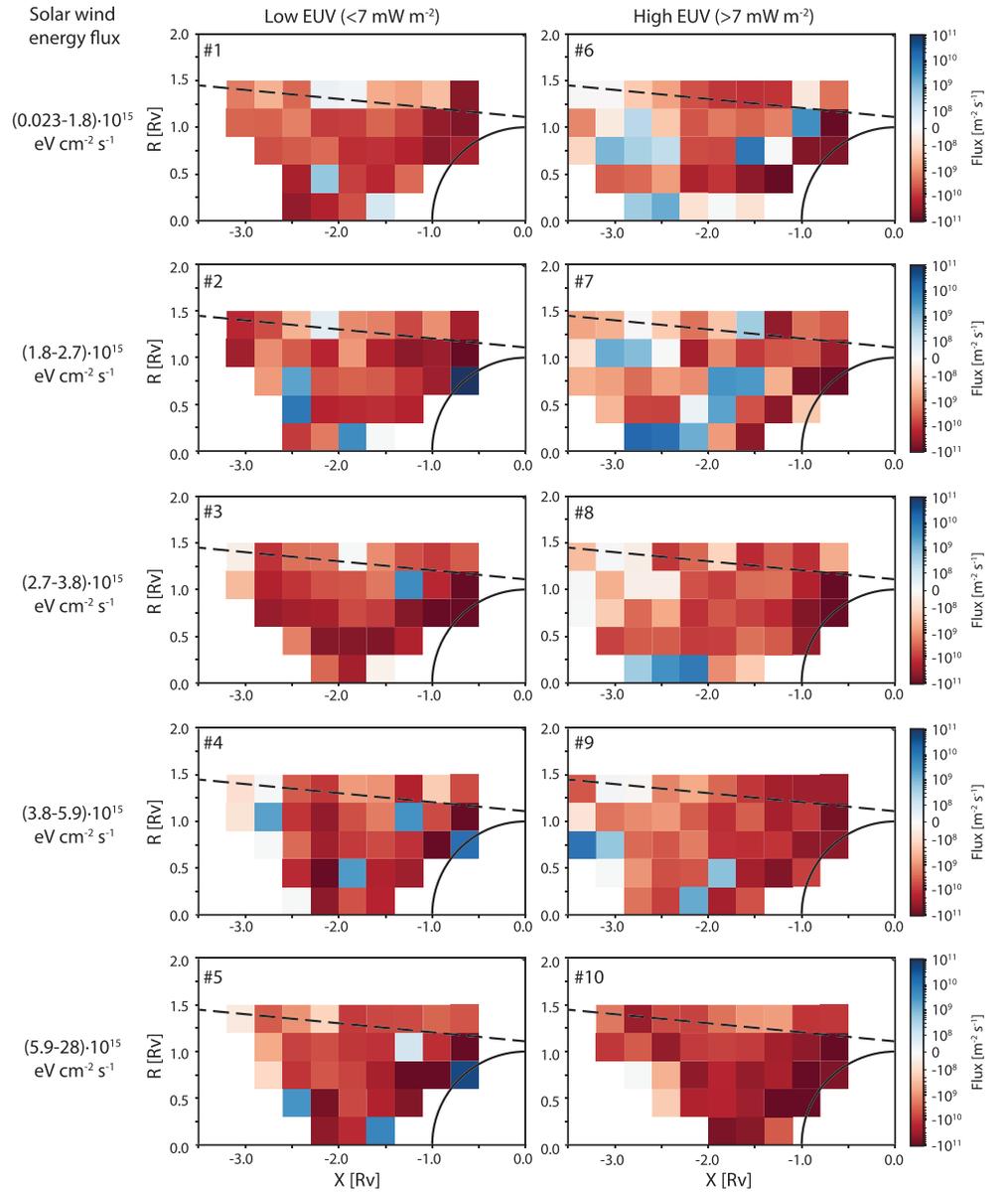
Figure 2. Maps of the O$^+$ flux in the Venusian plasma environment in cylindrical VSO coordinates, for each case of upstream parameters used in this study. The color depicts the flux in the X_{VSO} direction, where reddish bins represent tailward flux and blueish bins represent Venusward flux. The total escape rate calculated for each case #1–10 is tabulated in Table 1.

The net escape rate is then calculated from the flux $F_x(X_i, R_j)$ as

$$Q_{O^+} = \sum_i \frac{1}{N_i} \sum_j F_x\left(X_i, R_j\right) 2\pi R_j \Delta R,$$

where N_i is the number of slices used in the X direction, R_j is the radius of the center of the spatial bin used, and ΔR is the radial width of the spatial bin. The escape rates are calculated from the bins in the interval $X = [-2.3, -1.4]\ R_V$ and $R = [0, 1.2]\ R_V$. The calculated net escape rates for each of the 10 chosen upstream conditions is shown in Table 1.

Table 1
Calculated Average Escape Rates With Standard Errors for All Upstream Solar Condition Cases Studied[a]

#	$F_{SW,energy}$ $(10^{15}$ eV m^{-2} s$^{-1})$	I_{EUV} (mW m^{-2})	Q_{O+} $(10^{24}$ s$^{-1})$
1	0.023–1.8	<7	1.3 ± 0.2
2	1.8–2.7	<7	2.2 ± 0.7
3	2.7–3.8	<7	2.8 ± 0.6
4	3.8–5.9	<7	2.8 ± 0.6
5	5.9–28	<7	4.9 ± 0.2
6	0.023–1.8	>7	2.2 ± 0.8
7	1.8–2.7	>7	1.1 ± 0.4
8	2.7–3.8	>7	0.9 ± 0.3
9	3.8–5.9	>7	2.0 ± 0.5
10	5.9–28	>7	4.5 ± 0.7
11[a]	4–16[b]	>7	6–50

[a]Case #11 is the estimated average PVO condition, plotted in Figure 3.
[b]Estimated from McEnulty (2012).

3. Upstream Parameter Dependence for the O$^+$ Escape Rate

Figure 3 shows the escape rates of O$^+$ from Venus through the magnetotail and its dependence on the solar wind energy flux and solar EUV radiation flux. The escape rates are also tabulated in Table 1. The average escape is ~2·10^{24} s^{-1}, which is close to the range of previous studies using VEx/IMA measurements at (3–6)·10^{24} s^{-1} (see review in Futaana et al., 2017). The dependence on the upstream parameters is fitted with a power function $Q_{O+} = Q_0 \cdot F^\alpha$ for the solar wind energy flux and for high and low solar EUV flux respectively, to investigate the strength of the dependences.

From Figure 3, we clearly see that the O$^+$ escape rate increases with increasing solar wind energy flux, where the fitted logarithmic function to the high and low EUV conditions respectively gives the same relation $Q_{O+} \propto F_{energy,SW}^{0.5\pm0.3}$, where $Q_0 = 7.1\cdot10^{16}$ for high EUV and $Q_0 = 8.5\cdot10^{16}$ for low EUV. However, for the high EUV case, we note a v-shaped trend at the lowest solar wind energy cases. Further investigations show that this is indeed a real trend, and the escape is higher for the lowest solar wind energy flux. The detailed physics of this trend and the escape rates will be investigated in a future study. However, we deem that a slightly higher trend, but still within the upper boundary of the error on the fitted line, may be more representative as we move toward higher solar wind energy fluxes at the earlier history of Venus. Nevertheless, these results indicate that the escape of planetary ions is dependent on the amount of available energy in the solar wind and that energy is transferred through the induced magnetosphere boundary to the atmospheric particles. To escape the planet, the planetary ions need to reach escape velocity (~10 km/s). With an increase in transferred energy from solar wind to atmospheric particles, more ions can reach above the escape velocity and escape the planet. Even with the clear dependence, the relation is quite weak, with a small increase in the escape rate as the solar wind energy flux increases. This is in agreement with previous discussions of the escape rates during solar minimum (Fedorov et al., 2011), solar minimum and maximum (Masunaga et al., 2019), and during high dynamic pressure events such as interplanetary coronal mass ejections (ICMEs) and corotating interaction regions (CIRs) which only increased the escape rates by a factor 1.9 (Edberg et al., 2011).
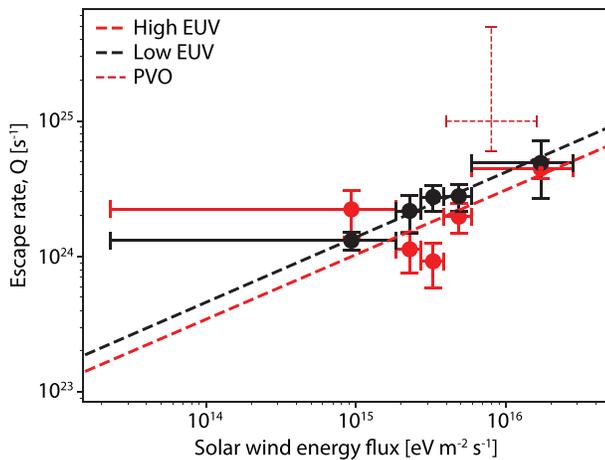
On the other hand, the results indicate that the escape rate only have a weak dependence on the solar EUV flux. The trend is almost the same for the low and high EUV conditions, where the escape rate is on average a factor <2 lower for the high solar EUV flux compared to the low solar EUV flux. As the EUV flux itself does not change more than a factor of 2 between the high and low cases, a weak dependence is not surprising. However, a decrease in escape rate with increasing solar EUV flux is opposite the general idea that an increase in production leads to increased material that can and will escape. This is explained by an increased fraction in the Venusward-directed flow during the solar maximum, as stated previously (Masunaga et al., 2019; Persson et al., 2018). The trend of increased return flows is also clear in Figure 2, where the number of blueish bins that indicate a major component toward Venus is increased from low to high solar EUV flux. In addition, as the solar EUV flux is the main source for ion production, an increase in the EUV leads to an increase in the number of ions that can potentially escape the planet. Therefore, the results can also imply that all ions that are produced cannot escape through the magnetotail. Presumably, with more ions in the ionosphere, the energy available will be shared between more ions which may decrease the average velocity per ion. Even though there are more ions, there will be a smaller percentage above the escape velocity (~10 km/s) which may lead to an insignificant change in the total escape rate.

Figure 3. The escape rate for each of the five separated ranges of solar wind energy flux using high and low EUV flux. The vertical error bars show the standard error of the escaping flux, and the horizontal error bars show the range for each upstream condition used to calculate the escape rates. The dashed lines present the best fit of a logarithmic function to the escape rate; $Q_{O+} = Q_0 \cdot F_{energy,SW}^{0.5\pm0.3}$, where $Q_0 = 7.1 \cdot 10^{16}$ for high EUV and $Q_0 = 8.5 \cdot 10^{16}$ for low EUV. The added red dashed cross shows the range of the escape rates determined from the PVO measurements (Brace et al., 1987; McComas et al., 1986) and the estimated average range of solar wind energy flux during the PVO era (McEnulty, 2012).

As the largest ion production is on the dayside, by solar EUV radiation ionization, the ions need to be transported from the dayside to the nightside in order to escape down the magnetotail. This transport may be a limiting factor for the total escape rate. A large day-to-night flow of ions with ~5 km/s was measured in the equatorial terminator region (Knudsen et al., 1980). Assuming the same flow over the full disk of Venus, the flow accounts for a transport of up to $5 \cdot 10^{26}$ O^+/s from dayside to nightside (Knudsen & Miller, 1992), though the flow in the north pole terminator region was recently found to have a more complex behavior, with a significant flow along the terminator (Persson et al., 2018). Taking into account that the flow is not uniform over the entire disk, the total flow from dayside to nightside is likely smaller than $5 \cdot 10^{26}$ O^+/s. In addition, a significant portion of the ions flowing into the nightside contributes to the nightside ionosphere (Knudsen & Miller, 1992). Even so, the flow is likely substantial enough to not limit the total escape rate from the Venusian atmosphere.

Escape rate results from the PVO mission are also included in Figure 3, ranging from $6 \cdot 10^{24}$ (McComas et al., 1986) to $5 \cdot 10^{25}$ s^{-1} (Brace et al., 1987), although the upper limit is likely overestimated by at least a factor 5 (Fedorov et al., 2011). The average solar wind energy flux was estimated from the solar wind velocity and density distributions from PVO measurements shown by McEnulty (2012). It is clear that the average solar wind energy flux was higher during the PVO era than the VEx era. In general, the escape rates from the PVO mission are consistent with the expected from our fitted logarithmic function within a factor of 2 difference (see Figure 3). In addition, the studies from the PVO era did not take into account that there is a significant return flow in the magnetotail, which decreases the total escape rates.

Measurements during extreme solar events, such as ICMEs, show that the local O^+ flux at above escape velocity can increase as much as 100 times the nominal flux (Luhmann et al., 2007). It is important to take into account that it is challenging to get the full picture from only one measurement point, during such transient events, and estimate the increase in the total escape rate. Edberg et al. (2011) showed that, on average, the escape rate in the magnetotail region increases by a factor 1.9 during high dynamic pressure transient events. Indeed, our results agree, where from medium solar wind energy flux to high solar wind energy flux conditions, the escape rates increase by a factor 1.9 for the low EUV radiation case. The high EUV radiation flux case shows an even larger increase of a factor 3.8 from medium to high solar wind energy flux. The detailed physics of the escape rate will be investigated in a future study.

These results indicate that the ion escape process at Venus is energy limited; i.e., the amount of energy input to the ionosphere is limiting the total escaping ion flux from the planet. Compare this to Mars, which was found to be source limited, i.e., almost all ions supplied to the region energized by the solar wind gain sufficient energy to escape, and so the ion production rate limits the supply and thus the total escaping flux, rather than the amount of energy available (Ramstad, Barabash, Futaana, Nilsson, et al., 2017). This may be explained by the fundamental difference in the size and gravity of Venus and Mars leading to an escape velocity twice as high on Venus (~10 km/s) compared to Mars (~5 km/s). The results can also be compared to results of ion escape from Earth. Schillings et al. (2019) investigated the influence of the solar dynamic pressure and solar EUV flux on the O^+ escape rates and found that the escape in the plasma mantle is positively correlated with the dynamic pressure, but there is a very small correlation with the solar EUV flux. A comparison between Earth and Venus is complex due to fundamental differences between the planets, which include, but are not limited to, the presence of an intrinsic magnetic field and the atmospheric composition (e.g. Gunell et al., 2018). However, the similar escape velocities (~10–11 km/s) and the similarity in the dependence on the upstream parameters indicate that both Earth and Venus have an energy-limited escape, while the smaller Mars have a source-limited escape. Nevertheless, a direct comparison between the escape rates is challenging, and we look forward to new advances in the field of planetary escape comparisons in future studies.

4. Total Escape Over 3.9 Ga

The logarithmic relations between the escape rate and the solar wind energy flux can be used to extrapolate the escape rates backwards in time. In order to make the extrapolation, information on the evolution of the solar wind is needed. The solar wind flux at the Venusian orbital distance can be calculated from the mass loss rate evolution of the Sun. From the absorption of the Lyman-α emission line measured for astrospheres of stars similar to the Sun, the mass loss rates are estimated and used to interpolate the solar mass loss rate
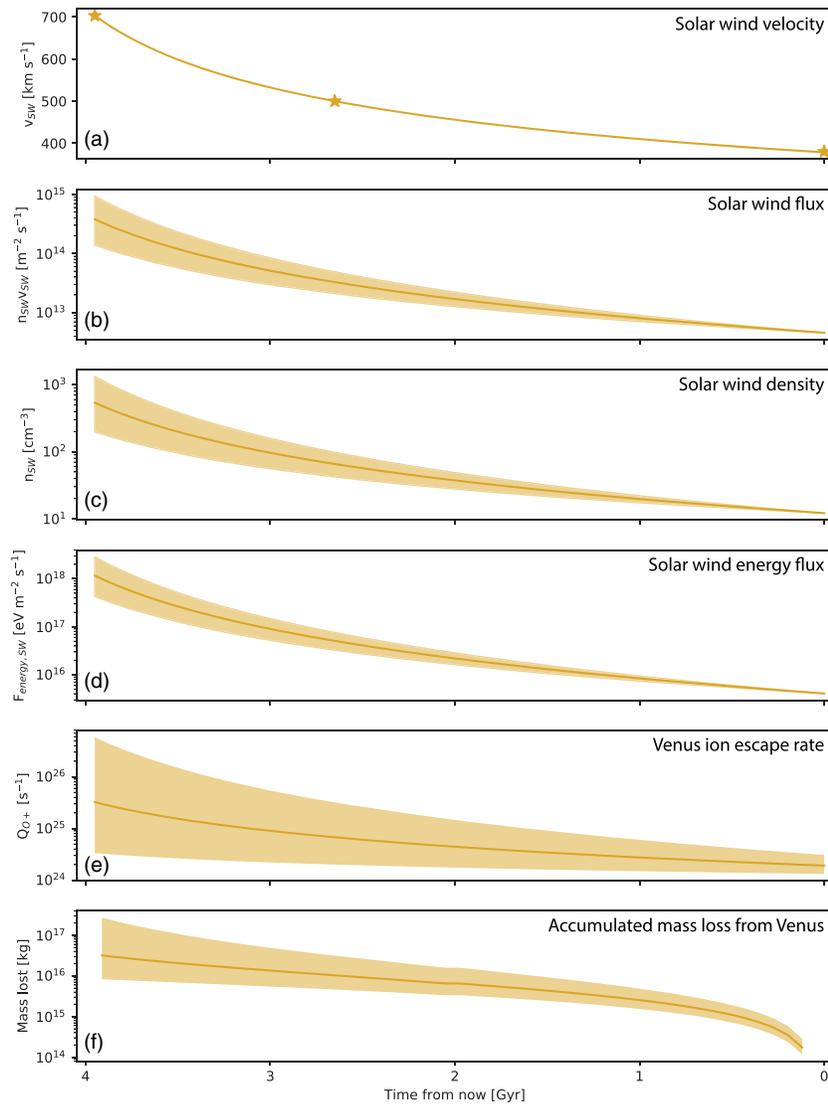
Figure 4. Evolution of upstream parameters over the past 3.9 Ga and the corresponding ion escape from Venus. (a) Solar wind velocity (where the stars represent the velocities reported in Airapetian & Usmanov, 2016), (b) solar wind flux, (c) solar wind density, (d) solar wind energy flux, (e) ion escape from Venus using the fitted dependence on solar wind energy flux, and (f) accumulated mass lost from Venus through ion escape over the past 3.9 Ga. The error on the solar wind parameters is propagated from the error on the mass loss evolution of our Sun (Wood, 2006), and the error on the escape and mass loss is from both errors on upstream parameters and error on the fitted escape.

back to ~3.9 Ga, $\dot{M} \propto t^{-2.33\pm0.55}$ (Wood, 2006). To extract the solar wind energy flux for the extrapolation, the evolution of the solar wind velocity is needed. From an MHD model of the solar wind, Airapetian and Usmanov (2016) estimated the solar wind speed at 0.7 Gyr, 2 Gyr, and today (stars in Figure 4a). We used a logarithmic fit to interpolate between these solar wind speeds and estimate the evolution of the solar wind velocity over the past 3.9 Ga (Figure 4a). With the solar wind velocity and flux, the solar wind energy flux is calculated (Figure 4d), which provides the evolution of the atmospheric ion escape from Venus over the past 3.9 Gyr (Figure 4e). Due to the weak relation between the solar wind energy flux and the escape rate, the escape rate only increases by about one order of magnitude to $Q_{O^+}(3.9 \text{ Ga}) = 3.2 \cdot 10^{25}$ s^{-1}, with a 1σ confidence interval of $[3.4 \cdot 10^{24}, 5.8 \cdot 10^{26}]$ s^{-1}.

As there is no clear trend on the EUV flux relation with the escape, for the EUV range of this data set, this relation has not been included in the extrapolation. However, earlier in the solar history, the EUV flux was 10–1,000 times stronger than it is today (Ribas et al., 2005; Tu et al., 2015). This would mean a significant

increase in the local ion production in the Venusian dayside upper atmosphere and potentially a significant increase in the returning ion fluxes. The increase in solar flux would also heat up the atmosphere, causing an expansion of the thermosphere (e.g., Erkaev et al., 2013; Johnstone et al., 2018) and cause an increase in the neutral thermal escape of H, which would also create a drag force on O that can cause neutral oxygen escape. A higher EUV flux may also photodissociate more CO_2 in the upper atmosphere, which increases the altitude of the exobase additionally as there would be less cooling of the upper atmosphere from CO_2 emissions (e.g. Johnstone et al., 2018; Tian et al., 2009). A higher exobase altitude, due to a higher heating rate from a stronger solar radiation or a change in atmospheric composition, could lead to an increase in the O^+ pickup ion rate as a larger portion of the neutral atmosphere is exposed to the solar wind, leading to an increase of the escape in the magnetosheath. On the other hand, with an increased ion production, the conductivity of the ionosphere would increase, which leads to stronger induced magnetic fields, and the ionosphere would more easily be able to resist the dynamic pressure of the solar wind, leading to an increased size of the induced magnetosphere. Depending on which of the effects of the increase in exobase and induced magnetosphere boundary altitudes are strongest, the escape would either increase or decrease. Although a larger induced magnetosphere would also increase the area over which the solar wind energy can be transferred to the Venusian atmosphere. A detailed study on the coupling between the incoming solar wind energy and the ion escape is planned. Nevertheless, using a dry 96% CO_2 atmosphere for Venus, Kulikov et al. (2006) showed that the largest increase in the O^+ pickup rate happened before 3.9 Ga where the effect of the increased EUV flux would have been largest. In this study, similarly to Kulikov et al. (2006), we assume that the composition of the atmosphere did not change significantly over the past 3.9 Ga. Effects from the EUV rate on the atmospheric evolution for Venus cannot be inferred from available measurements of the current escape rates at Venus; instead, substantial modeling is needed, and thus an elaborate discussion on the EUV flux effect on the escape rate is out of scope for this study.

Using the escape rate extrapolation from the solar wind energy flux relation, the total accumulated mass escaped from Venus through ion escape to space is estimated (Figure 4f). To account for the full O^+ ion escape, an escape through the magnetosheath is included as 30% of the total escape (Masunaga et al., 2019). From the escape rate over the past 3.9 Ga, the total mass that escaped to space as ions is calculated as $3.2 \cdot 10^{16}$ kg (1σ confidence interval: [$8.3 \cdot 10^{15}$, $2.7 \cdot 10^{17}$]), which accounts for ~0.007% of the total current atmospheric mass of Venus of $4.8 \cdot 10^{20}$ kg, i.e., approximately 6 mbar (1σ confidence interval: [1, 50]) of the equivalent surface pressure at Venus (out of 93 bar). In other words, the results in this study indicate that heavy ion escape to space has not had a strong influence on the evolution of the Venusian atmosphere. This mostly agrees with Kulikov et al. (2006), who with modeling efforts show that from now to 3.9 Ga, less than 0.1 bar was lost through atmospheric O^+ escape, taking into account the evolution of the solar wind from Wood (2006) and solar EUV flux from Ribas et al. (2005). The total escaped mass is higher than in this study, as they for example use an increased altitude of the exobase, start with a higher present-day escape rate, and do not take into account the measured return flows in the magnetotail (Persson et al., 2018).

Another important comparison to make is with the total amount of water present in the Venusian atmosphere. If we assume that all the O^+ escaping over the past 3.9 Ga originated from water, which is probable since the escape rate ratio of H^+ and O^+ is 2, the stoichiometric ratio of water (Barabash, Fedorov, et al., 2007; Persson et al., 2018), we can calculate how much of that water could have escaped to space. This leads to a total mass of water lost from the atmosphere through nonthermal escape in the magnetotail of $3.6 \cdot 10^{16}$ kg or a global equivalent water layer of 0.1 m (1σ confidence interval: [0.02, 0.6]). Today the total water content in the atmosphere is $8 \cdot 10^{15}$ kg (Lecuyer et al., 2000), but the historical water content on Venus was presumably something between 1% to 100% of Earth's current water inventory leading to a water depth of between 4 and 525 m (Kulikov et al., 2006; Way et al., 2016). Therefore, the results indicate that the loss of oxygen, emanating from water, cannot be explained solely by escape to space. Some part of the oxygen could have ended up in the surface through oxidation of the surface materials (Albarède, 2009). However, the high pressure at the surface does not allow for a high diffusion of volatiles into the surface materials. Therefore, the diffusion of oxygen into the surface materials hardly account for the full loss of water content in the Venusian atmosphere (Gillmann & Tackley, 2014). To further understand the history of water in the Venusian atmosphere, the loss of hydrogen to space should be constrained, which due to the lighter mass is more challenging to determine and is therefore left for a future study. The results of the oxygen escape do indicate that either water was not as abundant in the Venusian early history as previously assumed, or some piece of the

understanding of the historical escape of atmospheric particles to space is still missing. A similar study at Mars, using ASPERA-3 on board Mars Express, an almost identical instrument suite as on VEx, indicates the same conclusions; the nonthermal escape of O^+ ions to space cannot account for the total loss of atmospheric content. An extrapolation of the current escape rates and its dependence on the upstream parameters lead to a total of up to ~10 mbar lost to space during the past 3.9 Ga (Ramstad et al., 2018). On the other hand, from the extrapolation of the escape rate measurements made from the first Martian year of the MAVEN mission (2015–2016), Jakosky et al. (2018) concluded that the loss of an extensive Martian atmosphere can be explained if it includes other escape channels than the nonthermal ion escape through the magnetotail. An important difference between Mars and Venus is again the size of the planet. There are more escape channels, mainly for the neutrals, acting on the Martian atmosphere that become important due to the lower escape energy at Mars.

This leads us to the important notion that the escape rate extrapolation can constrain only the trends inferred from the current interaction between the solar wind and the Venusian upper atmosphere. The historical behavior of the atmospheric escape from Venus and the effects of the upstream parameters cannot be predicted through the current study alone. A future event study of the Venusian escape rates during an extreme space weather event, such as was done on Mars (Ramstad, Barabash, Futaana, Yamauchi, et al., 2017) and Earth (Schillings et al., 2018), would further constrain the escape rates for the upper part of the solar wind energy flux range. In addition, a sophisticated study including modeling efforts of both the effect of varying upstream parameters on the interaction with the Venusian induced magnetosphere, and the evolution of the Sun and its parameters, together with the results from current measurements to calibrate the numbers, would provide additional understanding of the evolution of the escape from the Venusian atmosphere.

Future missions to Venus would also help us further constrain the effect of the escape on the Venusian atmospheric evolution. For example, multipoint measurements would both be able to provide a timed connection between the upstream parameters and the variations in the magnetotail, without the need of assuming quasi-stable upstream parameters as in this study, and give more details on the ionosphere-magnetotail coupling during a space weather event. A future mission containing a plasma consortium with high time resolution, low-to-medium energy, low altitude measurements, with an orbit such as the proposed EnVision mission (Ghail et al., 2017), would provide excellent measurements of the physical processes of the escape, from the ionosphere and out to the near tail. An extremely important part is to get measurements from a wider range of upstream parameters, such as a wider EUV range, in order to connect the measurements from PVO and VEx and get a better constraint on the extrapolation back in time. In short, we look forward to new plasma measurements in the future that can provide an even more detailed view on the solar wind-Venus interactions.

5. Conclusions

We have determined the current relation between the escape of O^+ through the magnetotail of Venus and the upstream solar wind energy flux and solar EUV flux. We have shown that the escape increases with increasing solar wind energy flux. Oppositely, an increase in the solar EUV flux decreases the escape rate by less than a factor 2, mainly coming from an increased fraction of return flows from high to low solar EUV flux. The weak relation with the EUV flux may be explained by the small variations in EUV flux over the used solar cycle.

To characterize the total O^+ ion escape from the Venusian atmosphere, we use the relation with the solar wind energy flux to extrapolate the escape rates back to 3.9 Ga. We find that the total escaping mass of O^+ is $3.2 \cdot 10^{16}$ kg. Assuming that all the O^+ originated from water, the total water escaped from the Venusian atmosphere over the past 3.9 Ga is then equal to ~0.1 m water depth if spread equally over Venus' surface. Therefore, the ion escape to space over the past 3.9 Ga cannot account for a historical massive terrestrial-like ocean on the Venusian surface. This indicates that either water was not as abundant in the Venusian early history as previously assumed, or some piece of the understanding of the historical escape is missing. For example, in this study, we assumed that the current atmospheric conditions have been present over the past 3.9 Ga. If this is not the case, as if the atmospheric composition or temperature changed significantly, the found relation between the solar wind energy flux and O^+ escape rates needs to be revised accordingly. Either another escape channel was significantly more important in the early history, or the

solar transient events were considerably more effective at stripping the atmospheric content from Venus. Either way, the current escape rates and their relation with the upstream solar wind conditions indicate that the escape of ions to space cannot fully explain the evolution of the water in the Venusian atmosphere.

References

Airapetian, V. S., & Usmanov, A. V. (2016). Reconstructing the solar wind from its early history to current epoch. *The Astrophysical Journal Letters*, *817*, L24. https://doi.org/10.3847/2041-8205/817/2/L24

Albarède, F. (2009). Volatile accretion history of the terrestrial planets and dynamic implications. *Nature*, *461*(7268), 1227–1233. https://doi.org/10.1038/nature08477

Barabash, S., Fedorov, A., Sauvaud, J. J., Lundin, R., Russell, C. T., Futaana, Y., et al. (2007). The loss of ions from Venus through the plasma wakes. *Nature*, *450*(7170), 650–653. https://doi.org/10.1038/nature06434

Barabash, S., Sauvaud, J.-A., Gunell, H., Andersson, H., Grigoriev, A., Brinkfeldt, K., et al. (2007). The Analyser of Space Plasmas and Energetic Atoms (ASPERA-4) for the Venus Express mission. *Planetary and Space Science*, *55*(12), 1772–1792. https://doi.org/10.1016/j.pss.2007.01.014

Brace, L. H., Kasprzak, W. T., Taylor, H. A., Theis, R. F., Russell, C. T., Barnes, A., et al. (1987). The ionotail of Venus: Its configuration and evidence for ion escape. *Journal of Geophysical Research*, *92*(A1), 15–26. https://doi.org/10.1029/JA092iA01p00015

Colin, L. (1980). The Pioneer Venus program. *Journal of Geophysical Research*, *85*(A13), 7575–7598. https://doi.org/10.1029/JA085iA13p07575

Collinson, G. A., Frahm, R. A., Glocer, A., Coates, A. J., Grebowsky, J. M., Barabash, S., et al. (2016). The electric wind of Venus: A global and persistent "polar wind"-like ambipolar electric field sufficient for the direct escape of heavy ionospheric ions. *Geophysical Research Letters*, *43*, 5926–5934. https://doi.org/10.1002/2016GL068327

Donahue, T. M. (1999). New analysis of hydrogen and deuterium escape from Venus. *Icarus*, *141*(2), 226–235. https://doi.org/10.1006/icar.1999.6186

Donahue, T. M., Grinspoon, D. H., Hartle, R. E., & Hodges, R. R. Jr. (1997). Ion/neutral escape of hydrogen and deuterium: Evolution of water. In S. W. Bougher, D. M. Hunten, & R. J. Phillips (Eds.), *Venus II: Geology, geophysics, atmosphere, and solar wind environment* (pp. 385–414). Tucson, AZ: Univ. of Arizona Press.

Dubinin, E., Fraenz, M., Fedorov, A., Lundin, R., Edberg, N., Duru, F., & Vaisberg, O. (2011). Ion energization and escape on Mars and Venus. *Space Science Reviews*, *162*(1-4), 173–211. https://doi.org/10.1007/s11214-011-9831-7

Edberg, N. J. T., Nilsson, H., Futaana, Y., Stenberg, G., Lester, M., Cowley, S. W. H., et al. (2011). Atmospheric erosion of Venus during stormy space weather. *Journal of Geophysical Research*, *116*, A09308. https://doi.org/10.1029/2011JA016749

Erkaev, N. V., Lammer, H., Odert, P., Kulikov, Y. N., Kislyakova, K. G., Khodachenko, M. L., et al. (2013). XUV-exposed, non-hydrostatic hydrogen-rich upper atmospheres of terrestrial planets. Part I: Atmospheric expansion and thermal escape. *Astrobiology*, *13*(11):1011–1029. PMID: 24251443, DOI: 10.1089/ast.2012.0957.

Fedorov, A., Barabash, S., Sauvaud, J. A., Futaana, Y., Zhang, T. L., Lundin, R., & Ferrier, C. (2011). Measurements of the ion escape rates from Venus for solar minimum. *Journal of Geophysical Research*, *116*, A07220. https://doi.org/10.1029/2011JA016427

Futaana, Y., Stenberg Wieser, G., Barabash, S., & Luhmann, J. G. (2017). Solar wind interaction and impact on the Venus atmosphere. *Space Science Reviews*, *212*(3-4), 1453–1509. https://doi.org/10.1007/s11214-017-0362-8

Ghail, R., Wilson, C., Widemann, T., Bruzzone, L., Dumoulin, C., Helbert, J., et al. (2017). EnVision: Understanding why our most Earth-like neighbour is so different, *arXiv e-prints*, arXiv:1703.09010.

Gillmann, C., & Tackley, P. (2014). Atmosphere/mantle coupling and feedbacks on Venus. *Journal of Geophysical Research: Planets*, *119*, 1189–1217. https://doi.org/10.1002/2013JE004505

Grinspoon, D. (1993). Implications of the high D/H ratio for the sources of water in Venus' atmosphere. *Nature*, *363*, 428–431. https://doi.org/10.1038/363428a0

Gunell, H., Maggiolo, R., Nilsson, H., Stenberg Wieser, G., Slapak, R., Lindkvist, J., et al. (2018). Why an intrinsic magnetic field does not protect a planet against atmospheric escape. *Astronomy and Astrophysics*, *614*, L3 (2018). https://doi.org/10.1051/0004-6361/201832934

Hartle, R. E., & Grebowsky, J. M. (1990). Upward ion flow in ionospheric holes on Venus. *Journal of Geophysical Research*, *95*(A1), 31–37. https://doi.org/10.1029/JA095iA01p00031

Ingersoll, A. P. (1969). The runaway greenhouse: A history of water on Venus. *Journal of the Atmospheric Sciences*, *26*(6), 1191–1198. https://doi.org/10.1175/1520-0469(1969)026<1191:TRGAHO>2.0.CO;2

Jakosky, B., Brain, D., Chaffin, M., Curry, S., Deighan, J., Grebowsky, J., et al. (2018). Loss of the Martian atmosphere to space: Present-day loss rates determined from MAVEN observations and integrated loss through time. *Icarus*, *315*, 146–157. https://doi.org/10.1016/j.icarus.2018.05.030

Jarvinen, R., Kallio, E., & Dyadechkin, S. (2013). Hemispheric asymmetries of the Venus plasma environment. *Journal of Geophysical Research: Space Physics*, *118*, 4551–4563. https://doi.org/10.1002/jgra.50387

Johnstone, C. P., Güdel, M., Lammer, H., & Kislyakova, K. G. (2018). Upper atmospheres of terrestrial planets: Carbon dioxide cooling and the Earth's thermospheric evolution. *Astronomy and Astrophysics*, *617*, A107. https://doi.org/10.1051/0004-6361/201832776

Knudsen, W. C., & Miller, K. L. (1992). The Venus transterminator ion flux at solar maximum. *Journal of Geophysical Research*, *97*(A11), 17,165–17,167. https://doi.org/10.1029/92JA01460

Knudsen, W. C., Spenner, K., Miller, K. L., & Novak, V. (1980). Transport of ionospheric O+ ions across the Venus terminator and implications. *Journal of Geophysical Research*, *85*(A13), 7803–7810. https://doi.org/10.1029/JA085iA13p07803

Kollmann, P., Brandt, P., Collinson, G. A., Rong, Z. J., Futaana, Y., & Zhang, T. L. (2016). Properties of planetward ion flows in Venus' magnetotail. *Icarus*, *274*, 73–82. https://doi.org/10.1016/j.icarus.2016.02.053

Kulikov, Y., Lammer, H., Lichtenegger, H., Terada, N., Ribas, I., Kolb, C., et al. (2006). Atmospheric and water loss from early Venus. *Planetary and Space Science*, *54*(13-14), 1425–1444. https://doi.org/10.1016/j.pss.2006.04.021

Lammer, H., Lichtenegger, H., Biernat, H., Erkaev, N., Arshukova, I., Kolb, C., et al. (2006). Loss of hydrogen and oxygen from the upper atmosphere of Venus. *Planetary and Space Science*, *54*(13-14), 1445–1456. https://doi.org/10.1016/j.pss.2006.04.022

Lecuyer, C., Laurent, S., & François, G. (2000). Comparison of carbon, nitrogen and water budgets on Venus and the Earth. *Earth and Planetary Science Letters*, *181*(1-2), 33–40. https://doi.org/10.1016/S0012-821X(00)00195-3

Luhmann, J. G., Kasprzak, W. T., & Russell, C. T. (2007). Space weather at Venus and its potential consequences for atmosphere evolution. *Journal of Geophysical Research*, *112*, E04S10. https://doi.org/10.1029/2006JE002820

Luhmann, J. G., Ledvina, S. A., & Russell, C. T. (2004). Induced magnetospheres. *Advances in Space Research*, *33*(11), 1905–1912. https://doi.org/10.1016/j.asr.2003.03.031

Masunaga, K., Futaana, Y., Persson, M., Barabash, S., Zhang, T., Rong, Z. J., & Fedorov, A. (2019). Effects of the solar wind and the solar EUV flux on O+ escape rates from Venus. *Icarus*, *321*, 379–387. https://doi.org/10.1016/j.icarus.2018.11.017

McComas, D. J., Spence, H. E., Russell, C. T., & Saunders, M. A. (1986). The average magnetic field draping and consistent plasma properties of the Venus magnetotail. *Journal of Geophysical Research*, *91*(A7), 7939–7953. https://doi.org/10.1029/JA091iA07p07939

McElroy, M. B., Prather, M. J., & Rodriguez, J. M. (1982). Loss of oxygen from Venus. *Geophysical Research Letters*, *9*, 649–651. https://doi.org/10.1029/0GPRLA0000090000006000649000001

McEnulty, T. R. (2012). Oxygen loss from Venus and the influence of extreme solar wind conditions, (Doctoral dissertation). Retrieved from UC Berkeley Library, CA, US. (http://digitalassets.lib.berkeley.edu/etd/ucb/text/McEnulty_berkeley_0028E_13126.pdf). Location: UC Berkeley, CA, US.

Nordström, T., Stenberg, G., Nilsson, H., Barabash, S., & Zhang, T. L. (2013). Venus ion outflow estimates at solar minimum: Influence of reference frames and disturbed solar wind conditions. *Journal of Geophysical Research: Space Physics*, *118*, 3592–3601. https://doi.org/10.1002/jgra.50305

Pérez-de-Tejada, H. (2001). Solar wind erosion of the Venus polar ionosphere. *Journal of Geophysical Research*, *106*(A1), 211–219. https://doi.org/10.1029/1999JA000231

Persson, M., Futaana, Y., Fedorov, A., Nilsson, H., Hamrin, M., & Barabash, S. (2018). H$^+$/O$^+$ escape rate ratio in the Venus magnetotail and its dependence on the solar cycle. *Geophysical Research Letters*, *124*, 4597–4607. https://doi.org/10.1029/2018JA026271

Persson, M., Futaana, Y., Nilsson, H., Stenberg Wieser, G., Hamrin, M., Fedorov, A., et al. (2019). Heavy ion flows in the upper ionosphere of the Venusian north pole. *Journal of Geophysical Research: Space Physics*, *124*, 4597–4607. https://doi.org/10.1029/2018JA026271

Persson, M., Futaana, Y., Ramstad, R., Masunaga, K., Nilsson, H., Hamrin, M., et al. (2020). Supplementary data for: "The Venusian atmospheric oxygen ion escape: Extrapolation to the early solar system". Dataset Zeonodo. https://doi.org/10.5281/zenodo.3689213

Ramstad, R., Barabash, S., Futaana, Y., Nilsson, H., & Holmström, M. (2017). Global mars-solar wind coupling and ion escape. *Journal of Geophysical Research: Space Physics*, *122*, 8051–8062. https://doi.org/10.1002/2017JA024306

Ramstad, R., Barabash, S., Futaana, Y., Nilsson, H., & Holmström, M. (2018). Ion escape from mars through time: An extrapolation of atmospheric loss based on 10 years of mars express measurements. *Journal of Geophysical Research: Planets*, *123*, 3051–3060. https://doi.org/10.1029/2018JE005727

Ramstad, R., Barabash, S., Futaana, Y., Nilsson, H., Wang, X.-D., & Holmström, M. (2015). The Martian atmospheric ion escape rate dependence on solar wind and solar EUV conditions: 1. Seven years of Mars Express observations. *Journal of Geophysical Research: Planets*, *120*, 1298–1309. https://doi.org/10.1002/2015JE004816

Ramstad, R., Barabash, S., Futaana, Y., Yamauchi, M., Nilsson, H., & Holmström, M. (2017). Mars under primordial solar wind conditions: Mars express observations of the strongest CME detected at mars under solar cycle #24 and its impact on atmospheric ion escape. *Geophysical Research Letters*, *44*, 10805–10811. https://doi.org/10.1002/2017GL075446

Ribas, I., Guinan, E. F., Güdel, M., & Audard, M. (2005). Evolution of the solar activity over time and effects on planetary atmospheres. I. High-energy irradiances (1-1700Å). *The Astrophysical Journal*, *622*(1), 680–694. https://doi.org/10.1086/427977

Schillings, A., Nilsson, H., Slapak, R., Wintoft, P., Yamauchi, M., Wik, M., et al. (2018). O$^+$ escape during the extreme space weather event of 4–10 September 2017. *Space Weather*, *16*(9), 1363–1376. https://doi.org/10.1029/2018SW001881

Schillings, A., Slapak, R., Nilsson, H., Yamauchi, M., Dandouras, I., & Westerberg, L.-G. (2019). Earth atmospheric loss through the plasma mantle and its dependence on solar wind parameters. *Earth, Planets and Space*, *71*(1), 70. https://doi.org/10.1186/s40623-019-1048-0

Taylor, F., & Grinspoon, D. (2009). Climate evolution of Venus. *Journal of Geophysical Research*, *114*, E00B40. https://doi.org/10.1029/2008JE003316

Taylor, F. W., Svedhem, H., & Head, J. W. (2018). Venus: The atmosphere, climate, surface, interior and near-space environment of an earth-like planet. *Space Science Reviews*, *214*, 35. https://doi.org/10.1007/s11214-018-0467-8

Thiemann, E. M. B., Eparvier, F. G., & Woods, T. N. (2017). A time dependent relation between EUV solar flare light-curves from lines with differing formation temperatures. *Journal of Space Weather and Space Climate*, *7*, A36. https://doi.org/10.1051/swsc/2017037

Tian, F., Kasting, J. F., & Solomon, S. C. (2009). Thermal escape of carbon from the early Martian atmosphere. *Geophysical Research Letters*, *36*, L02205. https://doi.org/10.1029/2008GL036513

Tu, L., Johnstone, C. P., Güdel, M., & Lammer, H. (2015). The extreme ultraviolet and X-ray sun in time: High-energy evolutionary tracks of a solar-like star. *Astronomy and Astrophysics*, *577*, L3. https://doi.org/10.1051/0004-6361/201526146

Way, M. J., Del Genio, A. D., Kiang, N. Y., Sohl, L. E., Grinspoon, D. H., Aleinov, I., et al. (2016). Was Venus the first habitable world of our solar system? *Geophysical Research Letters*, *43*, 8376–8383. https://doi.org/10.1002/2016GL069790

Wood, B. E. (2006). The solar wind and the sun in the past. *Space Science Reviews*, *126*(1), 3–14. https://doi.org/10.1007/s11214-006-9006-0

Woods, T. N., Eparvier, F. G., Bailey, S. M., Chamberlin, P. C., Lean, J., Rottman, G. J., et al. (2005). Solar EUV Experiment (SEE): Mission overview and first results. *Journal of Geophysical Research*, *110*, A01312. https://doi.org/10.1029/2004JA010765

Wordsworth, R. D., & Pierrehumbert, R. T. (2013). Water loss from terrestrial planets with CO_2-rich atmospheres. *The Astrophysical Journal*, *778*, 154. https://doi.org/10.1088/0004-637X/778/2/154

Zhang, T. L., Baumjohann, W., Du, J., Nakamura, R., Jarvinen, R., Kallio, E., et al. (2010). Hemispheric asymmetry of the magnetic field wrapping pattern in the Venusian magnetotail. *Geophysical Research Letters*, *37*, L14202. https://doi.org/10.1029/2010GL044020